Available online at www.sciencedirect.com

ScienceDirect

Physics Procedia 56 (2014) 782 – 790

Physics Procedia

8th International Conference on Photonic Technologies LANE 2014

# Macroscopic Surface Structures for Polymer-Metal Hybrid Joints manufactured by Laser Based Thermal Joining

Klaus Schricker[a,]*, Martin Stambke[a], Jean Pierre Bergmann[a], Kevin Bräutigam[a], Philipp Henckell[a]

[a]*Ilmenau University of Technology, Department of Production Technology, Neuhaus 1, 98693 Ilmenau*

**Abstract**

The increasing application of hybrid structures in component design and fabrication allows to constantly enhance the realization of lightweight potentials. Laser-based joining of metals to polymers can obtain a local bonding with high load bearing capability. During the process, the polymer gets molten by the energy input of the laser beam and penetrates into the structure of the metal surface by means of a defined joining pressure. Macroscopic structures on the metal surface, produced by cutting or laser processing, are possible surface treatments for achieving the polymer-metal joints. The optimal geometry and other key parameters for the macroscopic surface structures are only partially known at present, e.g. a rising structure density causes a higher load capacity. Based on grooves and drilled holes, as reference geometries, the depth (0.1-0.9 mm), width (0.3-1.1 mm), alignment angle, diameter (1.0 mm- 1.5 mm), structure density and penetration depth of the molten polymer were correlated to the separation force. The results allow an essential insight into the main effects of macroscopic structures on the mechanical joint properties and the material performance of the polymer during the process.


Peer-review under responsibility of the Bayerisches Laserzentrum GmbH

*Keywords:* laser joining; polymer-metal hybrid joints; lightweight design; surface conditions; surface structures

## 1. Introduction and State of the Art

Increasing requirements regarding lightweight design and applications are setting new standards for conventionally used fabrication processes, especially when joining hybrid structures. On the one hand, conventional

* Corresponding author. Tel.: +49-3677-69-2980 ; fax: +49-3677-69-1660 .
*E-mail address:* info.fertigungstechnik@tu-ilmenau.de, klaus.schricker@tu-ilmenau.de


Peer-review under responsibility of the Bayerisches Laserzentrum GmbH
doi:10.1016/j.phpro.2014.08.086

materials, e. g. steel or aluminum, are characterized by high strength and processability and associated with economic advantages. On the other hand, new materials like carbon fiber reinforced plastics (CFRP), enable new technical designs, concerning load direction, high stiffness and low density, but are also accompanied by high costs and challenges within the process management.

Joining of polymers to metals is possible by using a connecting element (e. g. screw, rivet), an adhesive (e. g. epoxy resin) or a thermal process (e. g. laser welding). Connecting elements have a negative impact to local stress peaks caused by the punctual connection. Adhesives show disadvantages concerning joint preparation and aging. Thus, a thermal process enables a local joint with a high load capacity without using any additional material. Especially laser joining has certain advantages over competitive processes because it can be applied locally, independent from the component geometry and with a defined energy input.

In the process, the polymer is molten at the boundary layer to the metal by the energy input of the laser beam, penetrates the surface structure with a defined joining pressure and thus wets the metal surface. After solidification, a joint between the polymer and the metal is formed. Two process arrangements, depending on the laser-transparency of the polymer joining partner, can be outlined. One option is to position the workpieces in a way, that the laser beam passes through the polymer and heats the metallic joining partner at the interface. A minimum transparency in the laser wavelength of 15 % [12] is required, whereby CFRP cannot be processed and the process leads to a higher thermal load of the polymer, because the absorption takes place at the contact area between polymer and metal. Another possibility is to target the laser beam at the opposite metal surface. Consequently, the resulting heat is conducted throughout the metal plate, which leads to a temperature increase in the joining zone.

Based on these process variations, investigations within several fields of research were analyzed: Heat sources (e. g. laser beam, ultrasonic welding, conductive heating) [4-6], materials science [2, 6], bonding mechanisms [16-18], long term stability [3, 14, 15], coatings (e. g. zinc [13]) and surface morphology [3, 10-11, 20-21]. Regarding the surface treatment, structuring by laser [3, 10, 20], pickling [22] and corundum-blasting is shown [1, 4]. On the one hand, the structure density was identified as a key parameter for various structures [10, 11, 20], but investigations on geometric variations only exist based on the respective process [4, 20]. On the other hand, a detailed description for the different surface treatments does not exist and the common parameters, e. g. arithmetical mean deviation or mean roughness, do not provide sufficient information for a generally valid description [1].

In this paper, the influence of geometric parameters for macroscopic structures on load capacity is examined and possibilities for a generally valid classification and description of an ideal surface structure are given.

## 2. Experimental Setup

The joining process was carried out using the experimental setup shown in figure 1. A fiber-coupled diode laser by Laserline (LDM 1000; $\lambda$ = 980 nm; $P_L$ = 1 kW; $Ø_{Laser}$ = 5 mm) was used on a 3-axis processing table. As base materials, aluminum EN AW 6082 (t = 1.5 mm; width = 100 mm; length = 75 mm) and Polyamid 6.6 (PA66; t = 2 mm; width = 100 mm; length = 75 mm) were used for the heat-conduction joining (lap joint, overlap = 20 mm). The clamping device ensures a constant surface pressure of 0.5 N/mm² within the joining zone. The laser was positioned in the middle of the overlap.

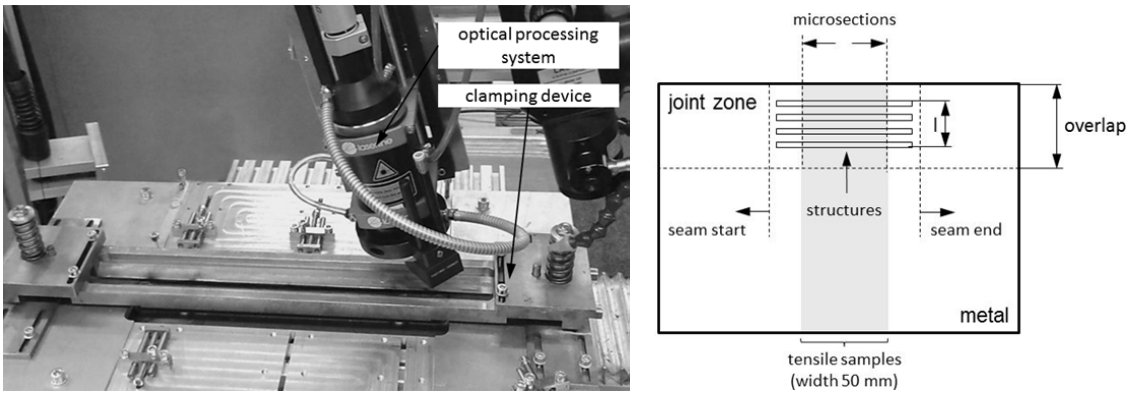


Fig. 1. Experimental setup and metal specimen (schematic design).

The metal specimen was designed as shown in figure 1. The seam start and seam end were not considered in the results because of process uncertainties caused by heat accumulation and the start-up phase. For this reason, the tensile samples and microsections (two per specimen) were taken out of middle of the joining zone. For mechanical testing, a modified tensile shear strength test was used in order to avoid a failure within the non-reinforced base material (figure 2). In this setup, the load was applied to the joining zone in terms of shear forces (test speed 10 mm/min).

A milling process was used for manufacturing the structures, because this process allows the preparation of defined geometries in various shapes without spill-over effects, e. g. deliberated undercuts. Thereby structure density (number of structures per area), depth (0.1-0.9 mm), width (0.3-1.1 mm) and alignment (0°, +45°, -45°) were examined for grooves. For evaluation, the polymer penetration behavior into the structures and the shear strength were examined (evaluation details are shown in figure 2, average penetration [mm²] from microsections). A statistical design of experiment (DoE, according to [19]) was set up. The DoE was designed by performing pretrials to determine the influence of the alignment (table 1, factor D), from which a $2^3$ experimental design was derived (table 1, factor A-C). According to the results, a second DoE was necessary in order to complete the investigations and was set up within the area of the highest shear strength (table 2, maximum of factors A-C). Both DoEs were verified by examinations on drilled holes (alignment 0 °; diameter 1.0…1.5 mm) regarding generally valid key figures for describing an ideal surface. All experiments were realized with identical parameters and referenced by examinations on corundum-blasted surface structures (grain size F60, see also [1]).

Table 1. Experimental Design – Stage 1.

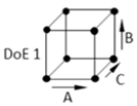


| factor | Name | entity | factor levels | | | |
|---|---|---|---|---|---|---|
| | | | - | 0 | + | |
| A | groove width | [mm] | 0,3 | 0,5 | 0,7 | |
| B | number of grooves | [1] | 1 | 3 | 5 | |
| C | groove depth | [mm] | 0,1 | 0,3 | 0,5 | |
| D | alignment | [°] | -45 | 0 | +45 | } pretrials |

Table 2. Experimental Design – Stage 2.

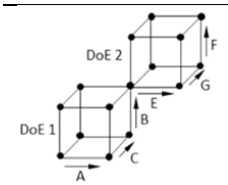


| factor | Name | entity | factor levels | | |
|---|---|---|---|---|---|
| | | | - | 0 | + |
| E | groove width | [mm] | 0,7 | 0,9 | 1,1 |
| F | number of grooves | [1] | 5 | 7 | 9 |
| G | groove depth | [mm] | 0,5 | 0,7 | 0,9 |

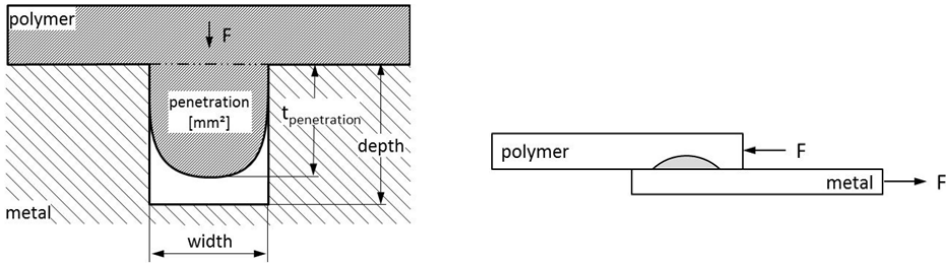


Fig. 2. Evaluation variables of polymer behavior (left) and shear strength test (right).

The investigations provide insights on generally valid key parameters characterizing the metal surface by the shear strength and the detailed consideration of the polymer behavior and relevant geometrical parameters. Thereby, the parameters in figure 3 are correlated to the load capacity to derive coherences between surface design and shear strength. The total structure surface (a), the stress bearing cross-section (b) and the projected area in load direction (c) were examined. The aspect ratio (structure depth / width) and the wetted surface were examined in abstracted investigations.

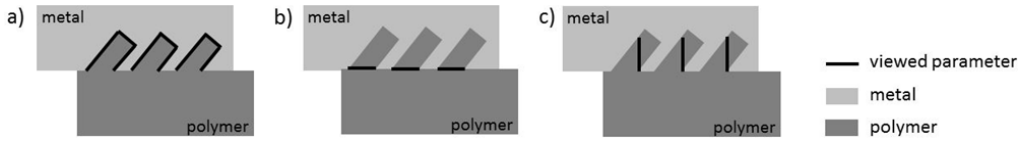


Fig. 3. Geometrical parameters.

## 3. Results and Discussion

### *3.1. Preliminary Investigations*

Based on preliminary investigations, the energy per unit length was varied in order to determine the optimal parameters compared to a corundum-blasted surface and transfer this knowledge on macroscopic structures. For the following experiments, the speed was set to 1.0 mm/s; in spite of the fact, that 0.5 mm/s achieves higher separation forces (figure 4) but at the same time causes severe thermal degradation. Considering the surface treatment for macroscopic structures, a pretrial with the alignment in loading direction was examined (comparable to factor level 0). Thereby, an alignment angle of -45 ° against loading direction achieved the highest load capacity. Furthermore, the effect of undercuts could be evaluated.

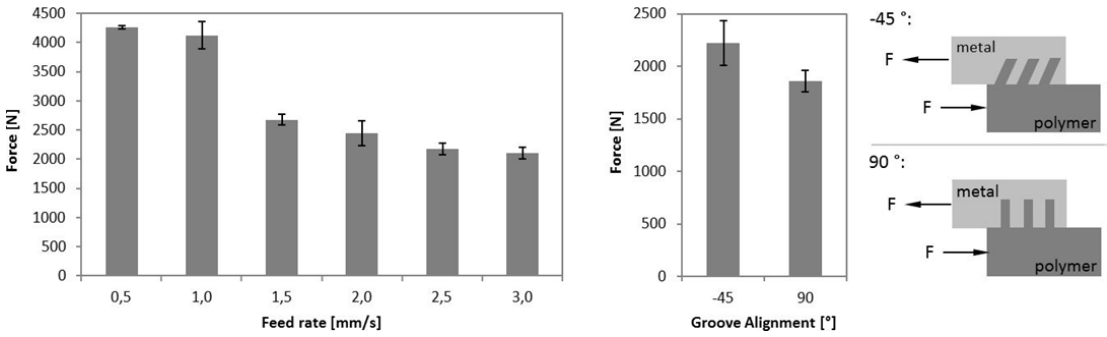


Fig. 4. Preliminary investigations on load capacity and groove alignment angle.

The penetration characteristics of the polymer into the metal surface across the lap joint is shown in figure 5 for a number of 9 grooves (maximum structure density) and varied geometric dimensions. For both graphs, the penetration depth increases towards the middle of the overlap up to a complete filling of the structure, but the edge is only filled partially because of less molten polymer in this area. This behavior is caused by the temperature distribution over the joint zone, whereas the temperature maximum occurs in the area of the absorbed laser beam ($ø_{Laser}$ = 5 mm). It is necessary to describe and regard the penetration characteristics dependent on the structure geometry, because the joint is only loadable in this area. Therefore, all experiments were realized with identical parameters to avoid an influence of viscosity or varying the amount of molten polymer in the joining zone.

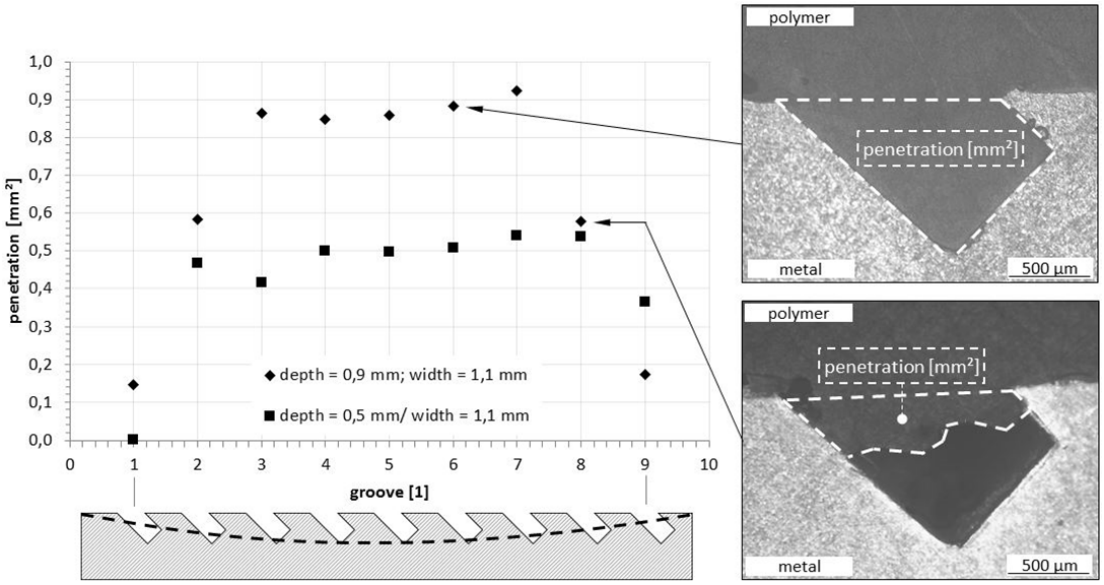


Fig. 5. Penetration characteristics of the polymer.

*3.2. Investigations on Geometrical Parameters and Polymer Penetration Characteristics for Grooves*

Based on the preliminary investigations, the interaction between the geometrical parameters and the shear strength as target figure was examined. The results were normally distributed; the level of significance is determined by the degree of freedom, the t-test, the effect size and the confidence interval and according to [19]. Thereby, the results of the first DoE (table 1) show, that depth, structure density and the interaction between depth and structure density are significant parameters (figure 6, stage 1). The interaction between width and depth can be reduced to the high significant influence of the depth. Furthermore, the insignificant impact of the width can be noticed. This is a first indicator, that the theoretical loadable area does not have an essential influence. The highest load capacity was achieved at the maximum factor levels (shear force F = 4.144 N), which led to the second DoE to be set up for further investigation (table 2).

The second DoE shows, that depth and number of grooves are significant parameters, whereas the interactions between number of grooves and depth and between width and depth, respectively, have no significant impact (figure 6, stage 2). The different t-value (2.145 to 2.13) is caused by an eliminated outlier in order to get normally distributed results. The highest shear strength (F = 6.120 N) occurs at the maximum factor levels (width = 1.1 mm; depth = 0.9 mm; number of grooves = 9). The width shows a low impact, e. g. the difference between a width of 0.7 mm and 1.1 mm by a maximum of depth and number of grooves is about 100 N and is within the experimental scatter. However, it should be noted, that the second DoE is set up to the point of the highest shear strength,

whereby interactions between the parameters can be less distinctive, which in turn explains their decrease of significance.

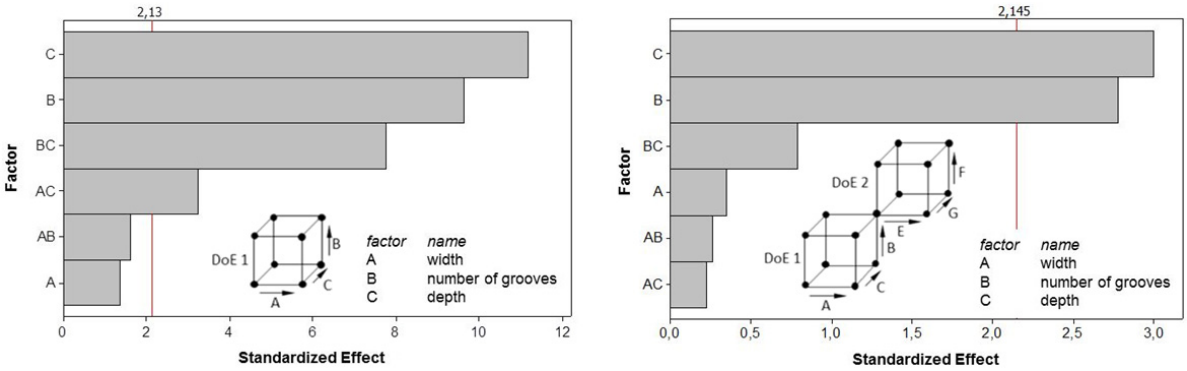


Fig. 6. Results of DoE: stage 1 (left) and stage 2 (right)

In summary, both DoEs show a significance of width and depth, the best results occur at the maximum factor levels. As expected, the structure density has a high impact. Nevertheless, the width shows an insignificant influence which is notable due to the stress bearing section. Furthermore, drilled holes (alignment angle 0 °) were examined to verify the results. These structures show a similar behavior; thereby a higher structure density causes higher shear forces. However, the diameter (comparable to the groove width) does not show any significant influence. Based on these results, an influence of the aspect ratio (depth / width) cannot be proven.

Assessing the polymer penetration characteristics, the penetration volume increases (average penetration [mm²] related to length 50 mm) with the volume of the grooves (width x depth related to length 50 mm) (figure 7, left). It was expected, that the penetration reaches a constant level because of the limited size of the melting layer, but sufficient molten polymer was provided due to time-temperature-regime. The difference between measured penetration and theoretical volume of the groove (Δpenetration) increases almost linear as well. Thus, the structures are not filled completely by molten polymer, but the load capacity reaches a constant level of 6.000 N indicated by overlapping standard deviations (figure 7, right). This assumed correlation between volume and load capacity cannot be transferred directly to drilled holes.

Furthermore, a consideration of a generally valid surface characterization of grooves and holes based on these results is necessary. Therefore, the geometrical parameters in figure 3 (Experimental Setup) were examined.

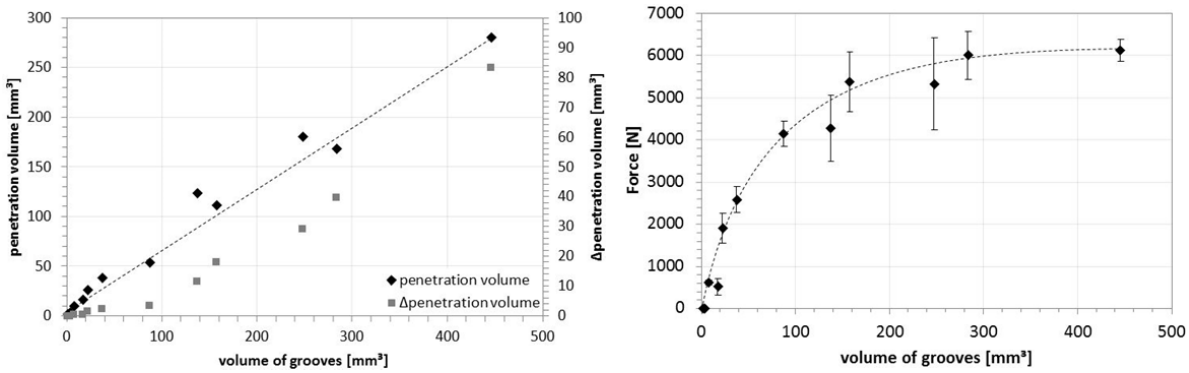


Fig. 7. Penetration volume dependent on groove volume (whole overlap, left) and correlation to shear force (right).

### *3.3. Key Parameters regarding Surface Characterization*

In the following plots, all examined structures were arranged together by using geometrical parameters, e. g. volume or surface of the grooves and holes. The combination of various structures to the same parameter occasionally causes high standard deviations, which need to be taken into consideration. First, a correlation between the surface of the grooves and holes and shear force is shown in the plot in figure 8. Hence it can be stated, that an increasing surface of grooves and holes causes higher shear forces. Both geometries show a tendency to similar behavior. For high shear forces, the overlapping standard deviations indicate the approach of a maximum value. This leads to the conclusion, that the total structure surface can be assumed as a possible indicator for the load capacity of a polymer-metal joint.

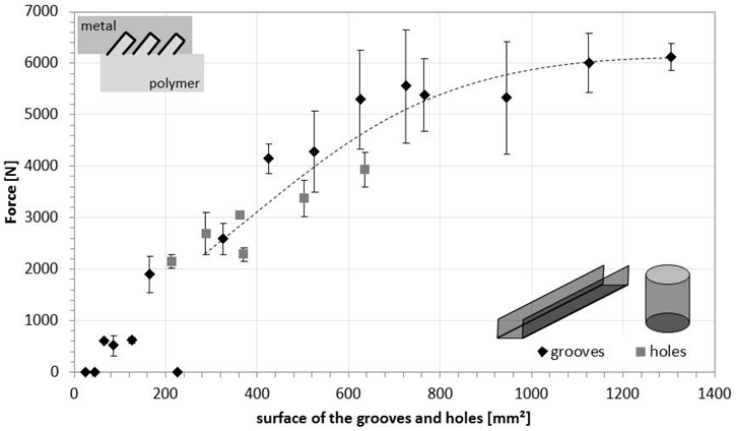


Fig. 8. Correlation between total structure surface and shear force.

In addition to these results, investigations show the influence of the joining section in loading direction, abstracted to the stress bearing cross section and the associated projected area. Both parameters are related to a specimen length of 50 mm. Finding a correlation was expected because of the test configuration (experimental setup, figure 2), the results are shown in figure 9. A correlation between the stress bearing cross section and shear force cannot be assumed, holes partially achieve much higher shear forces, although the grooves do not show a suitable behavior. A comparable view is obtained for the projected area in loading direction, but the holes do not fit into the excepted curve shape. In each case, the drilled holes achieve higher shear forces by increasing structure density and the diameter shows a minor influence as expected after the statistical design of experiments.

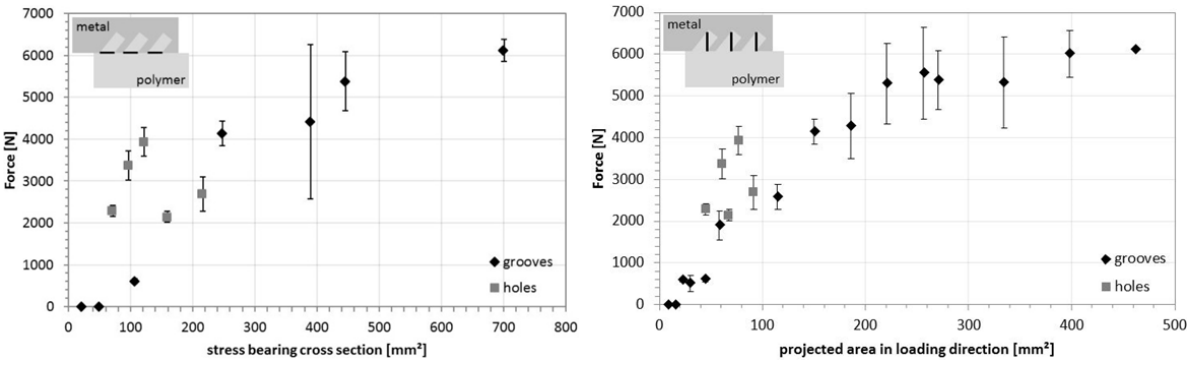


Fig. 9. Correlation between stress bearing cross section and shear force (left) and projected area in loading direction (right).

## 4. Summary and Outlook

Preliminary investigations provided results on ideal parameters for joining EN AW 6082 (corundum-blasted surface treatment) to PA66. These results were transferred to macroscopic structures and enable the assessment of an optimum alignment angle. On this basis, a statistical design of experiments determines the structure depth and structure density as significant parameters, whereby shear forces up to 6.1 kN can be reached by non-reinforced PA66. These results were validated on drilled holes.

Furthermore, key parameters regarding general surface characterization were examined. Thereby, the total surface of the grooves and holes, the stress bearing cross-section and the projected area in loading direction were linked to the obtained shear forces. The shear force could be correlated to the surface of the grooves and drilled holes, independent from geometry or alignment angle (grooves: -45 °; drilled holes: 0 °). The stress bearing cross section and projected area in loading direction do not allow a sufficient prediction for the load capacity.

Further investigations are necessary in order to transfer these results on microscopic structures, e. g. surface treatment by laser or corundum-blasting. Additionally, the assumed coherence between polymer penetration characteristics and shear strength for grooves has to be investigated further.

## Acknowledgements

The authors would like to thank the *Department of Economy, Employment and Technology (TMWAT)* in Thuringia (Germany) and the *European Social Fund (ESF)* for the support of the project *"Thermal Joining of Hybrid Structures"* (*"Thermisches Fügen von hybriden Materialkombinationen"*) in the research group *"Polymer Based Lightweight Composite Materials in Automotive Engineering"* (*"Kunststoffbasierte Leichtbauverbunde für Fahrzeuge"*, Förderkennzeichen 2011FGR0109).

Furthermore the authors would like to thank Dr. A. Eltze and company Laserline GmbH (Germany) for temporary supporting optical elements.

## References

[1] Bergmann, J. P.; Stambke, M., 2012: Potential of laser-manufactured polymer-metal hybrid joints. In: Physics Procedia 39, pp. 84-91
[2] Bergmann, J. P.; Schricker, K.; Stambke, M., 2013: Prozessbezogenes Benetzungsverhalten beim laserbasierten Fügen von hybriden Metall-Kunststoff-Verbunden. Tagungsband 9. Thementage Grenz- und Oberflächentechnik und 9. Thüringer Biomaterial-Kolloquium, 03.-05. Sept. 2013, pp. 70-74
[3] Amend, P.; Pfindel, S.; Schmidt, M., 2013: Thermal joining of thermoplastic metal hybrids by means of mono- and polychromatic radiation. Physics Procedia 41, pp. 98-105
[4] Flock, D., 2011: Wärmeleitungsfügen hybrider Kunststoff-Metall-Verbindungen. Rheinisch-Westfälische Technische Hochschule Aachen, PhD thesis
[5] Balle, F.; Wagner, G.; Eifler, D., 2007: Ultrasonic spot welding of aluminium sheet/carbon fiber reinforced polymer-joints. Materialwissenschaft und Werkstofftechnik, Bd. 38, Nr. 11
[6] Katayama, S.; Kawahito, Y.; Niwa, Y.; Kubota, S., 2007: Laser-assisted metal and plasitc joining. Proc. of 5th Laser Assisted Net Shape Engineering, pp. 41-51
[7] Katayama, S.; Jung, K.-W.; Kawahito, Y., 2010: High power Laser Cutting of CFRP, and Laser Direct Joining of CFRP to Metal. Proc. of 29th International Congress on Applications of Laser & Electro-Optics, pp. 333-338
[8] Bobzin, K.; Theiß, S.; Poprawe, R. et al., 2008: Der Exzellenzcluster „Integrative Produktionstechnik für Hochlohnländer" der RWTH Aachen University – Herstellung hybrider Metall-Kunststoffbauteile durch moderne Fügeverfahren. Joining Plastics, Nr. 03/2008, pp. 210-216
[9] Niwa, Y.; Kawahito, Y.; Kubota, S.; Katayama, S., 2008: Evolution of LAMP Joining Dissimilar Metal Welding. Proc. of 27th International Congress on Applications of Laser & Electro-Optics, pp. 311-317
[10] Holtkamp, J.; Roesner, A.; Gillner, A., 2010: Advanced in hybrid laser joining. Int. J. Adv. Manuf. Technol., pp. 923-930
In: Advanced Manufacturing Technology, Nr. 47/2010, pp. 923–930
[11] Flock D.; Haberstroh, E., 2010: Starke Verbindung ungleicher Partner. Kunststoffe, Nr. 11/2010, pp. 60-63, Carl Hanser Verlag
[12] Bayer Chemicals AG (Anmelder): Verfahren zum Verbinden von Formteilen aus Kunststoff und Metall; Europäische Patentanmeldung, Offenlegungsschrift, Patent-Nr. EP 1 508 398 A1

[13] Jung, K. W. et al., 2013: Laser direct joining of carbon fiber reinforced plastic to zinc-coated steel. Materials and Design; Nr. 47; pp. 179-188
[14] Roesner, A. et al., 2013: Long term stability of laser joined plastic metal parts. Physics Procedia; Nr. 41; pp. 169-171
[15] Mehner, A. et al., 2013: Corrosion of Aluminium Alloys in Integral Hybrid Components with Carbon Fiber Reinforced Plastics or Titanium. LightMAT Conference; Bremen
[16] Jung, K.-W.; Kwahito, Y.; Takahashi, M.; Katayama, S., 2013: Laser direct joining of carbon fiber reinforced plastic to aluminum alloy. Journal of Laser Applications, Vol. 25, Nr. 3
[18] Kawahito, Y.; Katayama, S., 2010: Innovation of laser direct joining between metal and plastic. Transactions of JWRI, Vol. 39, No. 2, pp. 50-52
[19] Kleppmann, W., 2001: Taschenbuch Versuchsplanung. Hanser Verlag
[20] Roesner, A.; Scheik, S.; Olowinsky, A.; Gillner, A.; Reigen, U.; Schleser, M., 2011: Laser Assisted Joining of Plastic Metal Hybrids. Physics Procedia 12, pp. 370-377
[21] Engelmann, C., 2013: Lasermikrostrukturen zum lasergestützen Fügen von Kunststoff und Metall. DVS-Congress, Essen
[22] Velthuis, R.; Mitschang, P.; Schlarb, A. K., 2005: Prozessführung zur Herstellung und Eigenschaften von Metall/Faser-Kunststoff-Verbunden. Institut für Verbundwerkstoffe GmbH, Kaiserslautern